JOURNAL OF GEOPHYSICAL RESEARCH, VOL. 104, NO. C4, PAGES 7641–7647, APRIL 15, 1999

Weakly nonlinear theory and sea state bias estimations

Tanos Elfouhaily[1] and Donald Thompson
Applied Physics Laboratory, Johns Hopkins University, Laurel, Maryland

Douglas Vandemark
NASA Goddard Space Flight Center, Wallops Island, Virginia

Bertrand Chapron
Institut Français de Recherche pour l'Exploitation de la Mer, Brest, France

Abstract. The theory of "weakly" nonlinear (WNL) waves is commonly used in generating higher statistical moments of a random surface wave field. These moments can be used, for example, to estimate the sea state bias (SSB) in radar altimetry under a geometric optical assumption. The present investigation suggests that several previous SSB studies appear to have misapplied this WNL theory by violating its condition of validity. As a result, a pronounced inconsistency appears even for lower-order moments. This inconsistency appears as a difference between the statistical moments of the nonlinear surface generated by the application of the WNL theory and those of the linear input (or bare) spectrum. If measured spectra, which yield measured moments (such as rms elevation and slope), are chosen as an input to WNL theory, then the corresponding moments of resulting output spectra may be severely overestimated. To strictly avoid the inconsistency, WNL theory must only be applied to long gravity waves where the wave-wave interactions are weak, hence the WNL epithet. To further illustrate this problem, we present an inversion scheme that determines the proper input spectrum by forcing the low-order moments of the output spectrum to equal the measured moments. Analytical solutions are given for this inversion based on an explicit formulation of the low-order nonlinear moments and a simplified one-dimensional power law spectrum. The solutions show that the high-frequency portion (wave components shorter than about 10 m) of the input (or bare) spectrum must be significantly less energetic than that of the output spectrum. Our results emphasize the importance of the shorter-scale waves in the SSB mechanism.

1. Introduction

As the use of satellite-borne altimeters becomes more common in many diverse fields of research and application, high-accuracy sea level measurements are becoming increasingly important. Of the several factors that can degrade the accuracy of these measurements, the sea state bias (SSB) is probably predominant [*Gaspar et al.*, 1994]. The SSB manifests itself in biasing the range reference below the actual mean sea level by several centimeters. In general terms, this bias can be attributed to the difference in electromagnetic backscattering from surface waves that have flat troughs and sharp crests. In the geometrical optics theory, the radar cross section at near-vertical incidence is proportional to the joint distribution of surface height and slopes (x and y components). The height is set at the location where the electromagnetic field touches the surface, and the slopes are set to satisfy the condition of specular scattering. Nonlinearities in water waves cause this joint distribution to depart from the well-known Gaussian (or normal) statistics [*Longuet-Higgins*, 1963]. This departure initiates the generation of higher moments, which in turn can be linked to the SSB via the skewness parameters [see *Jackson*, 1979]. While *Jackson* [1979] presented a one-dimensional example for a long-crested wave, *Srokosz* [1986] generalized both theory and technique to two-dimensional seas. Numerical evaluations of the SSB based on those theories were conducted by *Glazman and Srokosz* [1991] and *Glazman et al.* [1996].

The assumption of weak nonlinearity is commonly used in the study of ocean surface waves *Longuet-Higgins* [1963]. Our contention in the present work is that while the weakly nonlinear (WNL) theory is correct in form for long gravity waves, several previous studies have applied to cases where its validity conditions may be violated. *Longuet-Higgins* [1963] based his theory on the assumption that waves are "free," "undamped," and "weakly" nonlinear. Wave-wave interactions are limited to leading nonlinear order, hence the term weakly nonlinear. Application of this theory to shorter waves is implicitly equivalent to imposing these same restrictive conditions to those short waves that are driven by different physical mechanisms. Namely, for shorter waves, wave-wave interactions to higher orders become nonnegligible and must be accounted for. A correct generalization of WNL theory to higher orders and shorter waves can be found in papers by *Hasselmann* [1961, 1962a, b] and *Valenzuela* [1976].

[1]Also at University Space Research Association, NASA, Greenbelt, Maryland.

Paper number 1998JC900128.
0148-0227/99/1998JC900128$09.00

We suggest in this paper how it is possible to develop an inversion scheme that determines the required input wave spectrum such that the low-order moments of the output spectrum are consistent with measurements. Whereas only long waves should be included in the conventional WNL theory, our approach includes the effects of shorter waves. Expressions for the nonlinear variances carried to higher orders are given explicitly for the first time in this paper. The inversion scheme is then investigated for a one-dimensional spectrum to illustrate the inconsistency, in terms of spectral moments, of previous methods. Finally, we show that this inconsistency significantly impacts the SSB calculation.

Section 2 introduces linear and nonlinear equations for both the elevation and the velocity potentials as they were derived by *Longuet-Higgins* [1963] from the coupled hydrodynamic equations. Section 3 presents the difference between linear and nonlinear variances of both the elevation and slope variables. An inversion scheme is introduced and exercised using a simple, one-dimensional spectrum to illustrate why and how WNL theory has been overdriven in the past. Higher-order moments are given in section 4 along with an assessment of the degree to which the SSB is affected by the malfunctioning of WNL theory when shorter waves are included.

2. Nonlinear Formalism

The boundary conditions of the hydrodynamic problem of surface wave propagation can be solved by expanding the elevation and the velocity potential about a reference plane (i.e., $z = 0$) [see, e.g., *Hasselmann*, 1961]. The fluid is assumed to be irrotational, a condition that sets up a direct relationship between the velocity field and the gradient of a scalar potential. Both the elevation and potential can be expanded in a Taylor series in orders of the mode amplitudes. Hence elevation and potential are sums of elevations and potentials, respectively, at first order (linear), second order (first nonlinear), and higher orders. Thus the surface elevation $\zeta(\mathbf{r}, t)$ may be written as

$$\zeta(\mathbf{r}, t) = \zeta^{(1)}(\mathbf{r}, t) + \zeta^{(2)}(\mathbf{r}, t) + \cdots \tag{1a}$$

and the velocity potential $\phi(\mathbf{r}, z, t)$ as

$$\phi(\mathbf{r}, z, t) = \phi^{(1)}(\mathbf{r}, z, t) + \phi^{(2)}(\mathbf{r}, z, t) + \cdots \tag{1b}$$

where $\mathbf{r}$ is a horizontal vector, z is the vertical Cartesian coordinate, and t is time.

For a horizontally unbounded fluid of infinite depth with a free surface [$z = \zeta(\mathbf{r}, t)$], the first "linear" terms in these expansions are given by

$$\zeta^{(1)} = \sum_{n=1}^{N} a_n \cos \psi_n \tag{2a}$$

$$\phi^{(1)} = \sum_{n=1}^{N} b_n \sin \psi_n e^{-k_n z} \tag{2b}$$

where the phase ψ_n, the potential amplitude b_n, and the dispersion relationship for gravity waves in deep water are given by

$$\psi_n = \mathbf{k}_n \cdot \mathbf{r} - \omega_n t + \theta_n \tag{3a}$$

$$b_n = \frac{\omega_n}{k_n} a_n; \quad \omega_n = g|\mathbf{k}_n| \tag{3b}$$

with g being the gravitational acceleration. Equations (2a) and (2b) are termed linear since they are derived from a set of linear differential equations of elevation and potential at first order. Within the linear condition, a sample surface realization can be generated by summing over the appropriate wavenumber domain and selecting a different random draw for each mode amplitude a_n and mode phase θ_n. The amplitude a_n and phase θ_n are statistically independent random processes having Rayleigh and uniform distributions, respectively. In such a simulation, the wave troughs will not be as flat and the crests will not be as sharp as for real water waves. In particular, an electromagnetic scattering computation from this linear surface will not show any bias (SSB). Therefore, in order to study the SSB, higher orders of the nonlinear system are necessary.

Longuet-Higgins [1963] provided the leading nonlinear term in (1) as a double sum over a product of the mode amplitudes with a phase coupling as follows:

$$\zeta^{(2)} = \frac{1}{2} \sum_{i,j=1}^{N,N} a_i a_j (c_{ij} \cos \psi_i \cos \psi_j + s_{ij} \sin \psi_i \sin \psi_j) \tag{4a}$$

$$\phi^{(2)} = \frac{1}{2} \sum_{i,j=1}^{N,N} b_i b_j \left[\frac{B_{ij}^{+}}{\omega_i + \omega_j} \sin (\psi_i + \psi_j) e^{-|\mathbf{k}_i + \mathbf{k}_j| z} + \frac{B_{ij}^{-}}{\omega_i - \omega_j} \sin (\psi_i - \psi_j) e^{-|\mathbf{k}_i - \mathbf{k}_j| z} \right] \tag{4b}$$

where

$$c_{ij} = \frac{1}{\sqrt{k_i k_j}} [B_{ij}^{-} + B_{ij}^{+} - \mathbf{k}_i \cdot \mathbf{k}_j + (k_i + k_j) \sqrt{k_i k_j}] \tag{5a}$$

$$s_{ij} = \frac{1}{\sqrt{k_i k_j}} (B_{ij}^{-} - B_{ij}^{+} - k_i k_j) \tag{5b}$$

$$B_{ij}^{\pm} = \frac{(\omega_i \pm \omega_j)^2 (\mathbf{k}_i \cdot \mathbf{k}_j \mp k_i k_j)}{(\omega_i \pm \omega_j)^2 - \omega_{(\mathbf{k}_i \pm \mathbf{k}_j)}^2} \tag{6}$$

where $\omega_{(\mathbf{k}_i \pm \mathbf{k}_j)}^2$ is from the dispersion relationship equal to $g|\mathbf{k}_i \pm \mathbf{k}_j|$.

Adding these nonlinear terms to (1) produces a nonlinear surface that features flatter troughs and sharper crests, which are essential for analyzing the SSB. The question then becomes how accurately WNL theory reproduces the nonlinear aspect of a true surface. In other words, one should verify that inclusion of the first nonlinear order term is sufficiently realistic for free gravity wave representations. In the following section, statistical moments of this nonlinear process are derived to shed light on the applicability and relevance of WNL theory.

3. Second-Order Moments

3.1. Linear Derivation

Following *Longuet-Higgins* [1963], cumulants of the joint distribution of elevation ζ and slopes in two mutually orthogonal directions (ζ_x, ζ_y) can be expressed as integral sums over the two-dimensional surface spectrum. All first-order cumulants are zero because both elevation and slopes are zero-mean variables. Moments of any order not listed below are considered either zero or negligible. The second-order cumulants (or moments for a zero-mean process) are not zero, and they represent the "energy" contained in each process.

$$\kappa_{200} = \int_0^{k_c} F(\mathbf{k})\, d\mathbf{k} \tag{7a}$$

$$\kappa_{020} = \int_0^{k_c} (k^x)^2 F(\mathbf{k})\, d\mathbf{k} \tag{7b}$$

$$\kappa_{002} = \int_0^{k_c} (k^y)^2 F(\mathbf{k})\, d\mathbf{k} \tag{7c}$$

$$\kappa_{011} = \int_0^{k_c} k^x k^y F(\mathbf{k})\, d\mathbf{k} \tag{7d}$$

where κ_{mnl} is defined as the cumulants of the elevation and slope combination as $\zeta^n \zeta_x^m \zeta_y^l$ and k_c is the high-wavenumber cutoff. To keep the following equations simple, upper and lower limits will be dropped. It is understood that all the integral quantities in this paper are performed over wavenumbers up to the cutoff k_c.

Equations (7a)–(7d) have already been derived by numerous authors. We demonstrate in the following subsection that these moments are incomplete in the context of nonlinear processes.

3.2. Linear and Nonlinear Combined

The variances (or second-order moments for a zero-mean process) of the nonlinear processes are different than the ones derived under linear assumptions. The following analytic equations for both elevation and slopes are given here for the first time. An outline leading to the following equations can be found in the original paper by *Longuet-Higgins* [1963],

$$\kappa_{200} = \int F(\mathbf{k})\, d\mathbf{k} + \frac{1}{2}\int\int (c_{12}^2 + s_{12}^2) F(\mathbf{k}_1) F(\mathbf{k}_2)\, d\mathbf{k}_1\, d\mathbf{k}_2 \tag{8a}$$

$$\kappa_{020} = \int k^{x2} F(\mathbf{k})\, d\mathbf{k} + \frac{1}{2}\int\int (C_{12}^{x\,2} + S_{12}^{x\,2}) F(\mathbf{k}_1) F(\mathbf{k}_2)\, d\mathbf{k}_1\, d\mathbf{k}_2 \tag{8b}$$

$$\kappa_{002} = \int k^{y2} F(\mathbf{k})\, d\mathbf{k} + \frac{1}{2}\int\int (C_{12}^{y\,2} + S_{12}^{y\,2}) F(\mathbf{k}_1) F(\mathbf{k}_2)\, d\mathbf{k}_1\, d\mathbf{k}_2 \tag{8c}$$

$$\kappa_{011} = \int k^x k^y F(\mathbf{k})\, d\mathbf{k} + \frac{1}{2}\int\int (C_{12}^x C_{12}^y + S_{12}^x S_{12}^y) F(\mathbf{k}_1) F(\mathbf{k}_2)\, d\mathbf{k}_1\, d\mathbf{k}_2 \tag{8d}$$

where

$$C_{12}^i = k_2^i c_{12} - k_1^i s_{12} \tag{9a}$$

$$S_{12}^i = k_1^i c_{12} - k_2^i s_{12} \tag{9b}$$

with i representing either x or y. The assumptions under which (8a)–(8d) were derived are identical to those made by *Longuet-Higgins* [1963]. The important difference is that we keep higher-order terms even at this low order of the moments.

The double integrals in (8a)–(8d) result from the two-wave interaction imposed by stopping the expansion of the elevation and the velocity potential at second order in (1a) and (1b). One is tempted to neglect these double integrals by assuming that they should be much smaller than the leading single integral terms, but if so, then the second-order moments would merely be equal to the linear moments given by (7a)–(7d). Unfortunately, this assumption is only justified in certain particular cases. The condition of smallness of the double integral defines a stringent constraint, which can be translated as a compromise between short-wavenumber cutoff k_c and rms height ($\sigma_h = \sqrt{\kappa_{200}}$). This can be put into an inequality given as

$$k_c \sigma_h < 1. \tag{10}$$

So, if the sea state represented here by the significant wave height $H_s = 4\sigma_h$ is less then 4 m, say, then WNL theory is restricted to very long gravity waves [$k_c < 1$ rad/m from (10)]. Therefore only waves longer than about 6 m should be admissible into WNL theory.

In most of the previous studies, the double integrals were not included, even though the smallness condition was not satisfied. As a consequence, the omission of these extra terms in the elevation and slope variances may highly bias the results of the studies. This inconsistency manifests itself through an appreciable difference between the input surface spectrum (or bare spectrum) and the output spectrum (or measured spectrum). The former is used to simulate the surface, and the latter is deduced from the simulated surface itself. This inconsistency begins with the second-order moments as shown in (8) as opposed to (7a)–(7d).

Some previous studies have anticipated a breakdown of the weakly nonlinear theory in its nonlinear moments [see, e.g., *Barrick and Weber*, 1977; *Barrick and Lipa*, 1985; *Creamer et al.*, 1989]. The breakdown or inconsistency that we discuss in the present paper is fundamentally different because it even effects the linear moments. *Barrick and Lipa* [1985, p. 91] showed that the "coupling coefficient" A [*Weber and Barrick*, 1977] "saturates" beyond a certain wavenumber cutoff. This saturation only affects the third-order moments [see *Barrick and Lipa*, 1985, equation (22)]. The breakdown that we are considering causes the divergence of moments starting at second order and not a saturation of the third-order moments as suggested by *Barrick and Lipa* [1985].

The block diagram in Figure 1 sketches the process to recall the following obvious but important point: from the perspec-

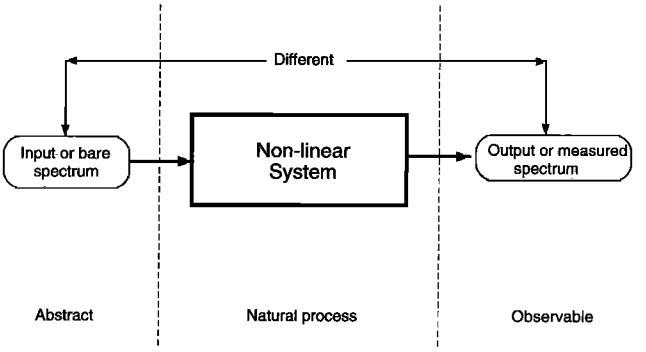

Figure 1. Block diagram showing how the output or measured spectrum differs from the input or bare spectrum in the general context of nonlinear systems. If the nonlinearities are "weak," then the output spectrum is equivalent to the input one with respect to low-order moment criteria.

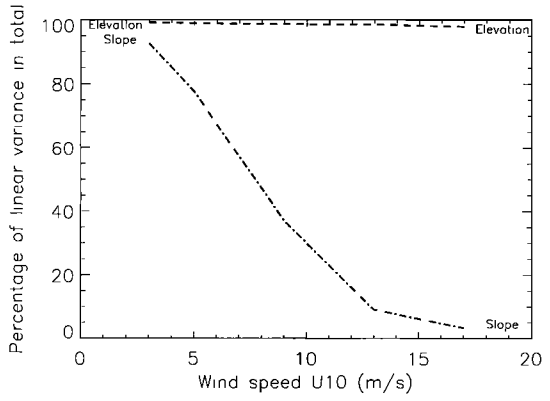

Figure 2. The two-dimensional spectrum of *Glazman et al.* [1996] used in the surface generation to illustrate the inconsistency. Nonlinear contribution to the slope variance is not negligible if waves as short as 40 cm are included. Omega is the inverse wave age defined as the ratio between the phase speed of the dominant wave and the wind speed ($\Omega = C_p/U_{10}$). Percentage of linear variance in total (linear + nonlinear) is shown versus wind speed at a height of 10 m from the surface in meters per second. Dashed line denotes elevation, and dash-dotted line represents unidirectional slope variance. While the linear elevation stays at about 99% of the total variance, the linear slope variance, however, could drop to as low as a few percent in the contribution to the total variance. The nonlinear part in the slope variance is clearly not negligible for this particular wave cutoff and those chosen wind speeds.

tive of statistical moments, the output is equivalent to the input only under weak nonlinearities. In the general case, however, the input and output spectra can become quite different. Figure 2 shows the percentage of linear variance (equations (7a)–(7d)) in the total variance (equations (8a)–(8d)) as a function of wind speed for the two-dimensional wave spectrum utilized by *Glazman et al.* [1996]. The corresponding high-wavenumber cutoff is set to 40 cm as proposed by *Glazman et al.* [1996]. The degree of development of the sea is represented by the inverse wave age ($\Omega = C_p/U_{10} = 1$, where C_p is the phase speed of the dominant wave peak and U_{10} is the wind speed at a height of 10 m above the surface), which in this case corresponds to a nearly fully developed sea. While the linear elevation term carries 99% of the total variance, the linear slope variance drops dramatically to as low as a few percent. The nonlinear contribution to the slope variance is clearly not negligible for this particular wave cutoff at wind speeds greater than 3 or 4 m/s. In fact, the double integral, which at first might be thought to be only a perturbation, provides 50% of the total slope variance for the most common open ocean wind speed of 7 m/s. Hence these results are highly contaminated by short gravity waves, which cannot be handled by WNL theory. Figure 3 is similar to Figure 2, but using a different two-dimensional spectrum (unified spectrum of *Elfouhaily et al.* [1997]). Figure 3 reinforces the point that the inconsistency is caused primarily by the misapplication of the theory and not because of the form of the chosen two-dimensional spectrum or its directional spreading. In the following subsections, we further demonstrate that the divergence arises from the fact that two spectra are needed at the same time, one at the input and a different one at the output of the simulation process.

The output spectrum is assumed to be measurable and representative of the actual sea surface. In clear contrast, the unknown input spectrum should only be recognized as the analytical function associated with the nonlinear transform.

3.3. Spectral Inversion

To further investigate the consequences of the inconsistency referred to above, one can envision finding a particular spectral form that guarantees compatibility with the measured statistical properties (i.e., low-order moments) of the simulated surface. With this property in mind, the moment equations (for the one-dimensional case) become

$$\int F_{in}(k)\,dk + \frac{1}{2}\int\int (c_{12}^2 + s_{12}^2) F_{in}(k_1) F_{in}(k_2)\,dk_1\,dk_2 = \int F_{out}(k)\,dk \tag{11a}$$

$$\int k^2 F_{in}(k)\,dk + \frac{1}{2}\int\int (C_{12}^2 + S_{12}^2) F_{in}(k_1) F_{in}(k_2)\,dk_1\,dk_2 = \int k^2 F_{out}(k)\,dk \tag{11b}$$

where the input or bare spectrum F_{in} is an unknown that must be deduced from the supplied observable spectrum F_{out}, which is assumed to be measurable and known. The coefficients $c_{1,2}$, $s_{1,2}$, $C_{1,2}$, and $S_{1,2}$ are determined by WNL theory (see (5a), (5b), (9a), and (9b)). We note that the low-order moments of F_{out} must be consistent with the measurable moments of a realistic surface governed by two-wave interactions. The input spectrum F_{in}, however, is a fictitious spectrum that represents ideal waves that cannot interact with each other. It is also clear that F_{in} is dependent on the number of interactions considered. In our case, only interactions to second order are considered, which forces F_{in}, after inversion, to be exclusively determined by two wave-wave interactions.

To keep the illustration relatively simple, we have chosen a one-dimensional Phillips spectral form given by

$$F_{in} = \beta_i k^{-n_i} \tag{12a}$$

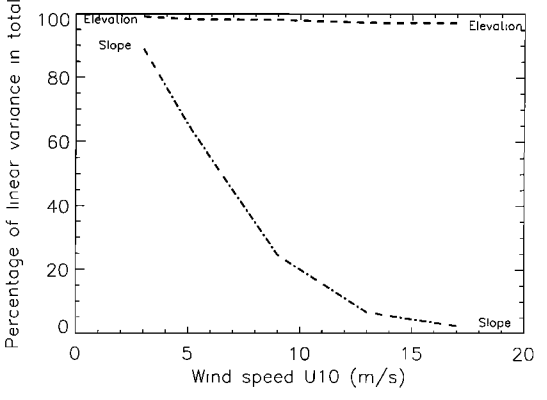

Figure 3. Same as Figure 2, but with the unified two-dimensional spectrum [*Elfouhaily et al.*, 1997], clearly showing that the inconsistency, lower percentages on the slope variance, are not caused by the original shape of the two-dimensional spectrum but, rather, in where to apply the spectrum in a nonlinear simulation.

$$F_{out} = \beta_o k^{-n_o} \tag{12b}$$

according to *Phillips* [1977]. The parameters β and n are assumed to be constant, although this choice is not necessarily representative of real waves on a water surface. The point here is to illustrate the inconsistency with a typical one-dimensional example without having to solve the general two-dimensional problem.

Equations (11a) and (11b) then reduce to

$$\beta_t H^{k_c}_{k_p}(-n_t) + \beta_t^2[G^{k_c}_{k_p}(-n_t, 2 - n_t) + G^{k_c}_{k_p}(2 - n_t, -n_t)] = \beta_o H^{k_c}_{k_p}(-n_o) \tag{13a}$$

$$\beta_t H^{k_c}_{k_p}(2 - n_t) + \beta_t^2[G^{k_c}_{k_p}(-n_t, 4 - n_t) + 6G^{k_c}_{k_p}(2 - n_t, 2 - n_t) + G^{k_c}_{k_p}(4 - n_t, -n_t)] = \beta_o H^{k_c}_{k_p}(2 - n_o) \tag{13b}$$

where k_p and k_c are the wavenumber peak and cutoff, respectively. The functions $H^{k_c}_{k_p}$ and $G^{k_c}_{k_p}$ are analytical functions given in the appendix.

The nonlinear system of (13a) and (13b) may be solved for the unknown amplitude and exponent of the input spectrum (β_t, n_t) for specified values of the corresponding output quantities (β_o, n_o). In particular, we have inverted this system for a peak wavenumber, $k_p = 0.2$ rad/m, and wind speed of about 7 m/s, and ($\beta_o = 5 \times 10^{-3}$, $n_o = 3$) corresponding to a (one-dimensional) *Phillips* [1977] spectrum. Figure 4 shows the inverted amplitude of the spectrum. The corresponding exponent of the one-dimensional spectrum is plotted in Figure 5. For high-wavenumber cutoff values k_c of 15 and 200 rad/m, we find that the parameters of the input spectrum must be $\beta_i = 3.0 \times 10^{-3}$, $n_i = 3.40$ and $\beta_t = 1.5 \times 10^{-3}$, $n_i = 3.95$, respectively. These high-wavenumber cutoff values were chosen in the SSB studies of *Glazman et al.* [1996] and *Jackson* [1979], respectively. We see from this example that for high values of k_c, one must use an input spectrum whose amplitude and slope are significantly different in order to obtain an output spectrum whose low-order moments are consistent with the measurements. It is reiterated that the Phillips spectral form has been chosen only for illustration. One could generalize the approach outlined above to any suitable output spectra. The main point we wish to emphasize is that for high-wavenumber cutoff values, the output spectrum derived from WNL theory must be significantly different from the input spectrum if the low-order moments are to remain unchanged.

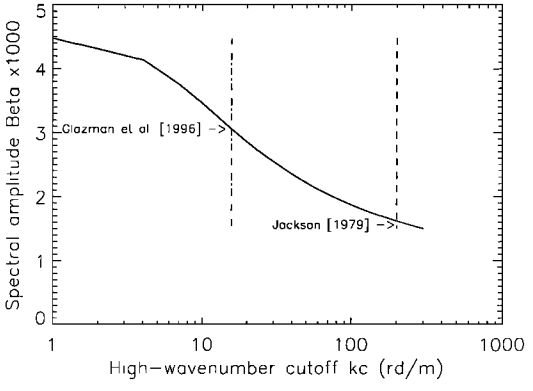

Figure 4. Inverted scale parameter β_t by imposing a Phillips output spectrum $\beta_o k^{-n_o}$ with $\beta_o = 5 \times 10^{-3}$ and $n_o = 3$. The results are displayed as a function of short wave cutoff for one peak wavenumber $k_p = 0.2$ rad/m.

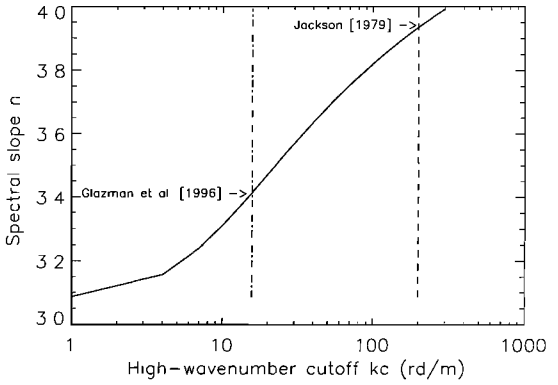

Figure 5. Inverted exponent parameter n_t for the same output spectrum as in Figure 4. Vertical lines indicate the corresponding spectral scale and exponent that *Jackson* [1979] and *Glazman et al.* [1996] should have used in order to obtain a spectrum of Phillips ($5 \times 10^{-3}\, k^{-3}$) as a result of the simulation.

4. Effect on Sea State Bias

This section establishes the link between the third-order moments and the sea state bias in order to illustrate one practical consequence of the inconsistent usage of WNL theory discussed above.

4.1. Third-Order Moments

We would like to know how much the SSB simulations are affected by the inconsistency revealed in the previous sections. To accomplish this goal, second-order moments are not sufficient; higher-order moments are required. The third-order moments are provided in the following equations:

$$\kappa_{300} = 3 \iint c_{12} F(\mathbf{k}_1) F(\mathbf{k}_2)\, d\mathbf{k}_1\, d\mathbf{k}_2 \tag{14a}$$

$$\kappa_{120} = \iint \alpha^{xx}_{12} F(\mathbf{k}_1) F(\mathbf{k}_2)\, d\mathbf{k}_1\, d\mathbf{k}_2 \tag{14b}$$

$$\kappa_{102} = \iint \alpha^{yy}_{12} F(\mathbf{k}_1) F(\mathbf{k}_2)\, d\mathbf{k}_1\, d\mathbf{k}_2 \tag{14c}$$

$$\kappa_{111} = \iint \alpha^{xy}_{12} F(\mathbf{k}_1) F(\mathbf{k}_2)\, d\mathbf{k}_1\, d\mathbf{k}_2 \tag{14d}$$

where

$$\alpha^{**}_{12} = (k_1^{**2} + k_2^{**2}) c_{12} - k_1^{**} k_2^{**} s_{12} \tag{15}$$

Those moments have already been derived by *Srokosz* [1986], though presented in discrete form. At this point we stress the fact that third-order cumulants of the slopes are zero and not required in this paper. Had we expanded the hydrodynamic equations to third order, we should have obtained nonzero third-order cumulants for the slope components. Thus non-Gaussian distributions of the slope components are driven by three-wave interactions or higher.

4.2. Induced Skewness

Again, for simplicity, we will provide a one-dimensional version of the problem using spectra of the Phillips form given by (12a) and follow a development similar to *Jackson* [1979] to compute the SSB. For a generalization of the SSB computation to two dimensions, the reader should refer to *Srokosz* [1986]. With these assumptions and restrictions we can use the results of the preceding section to write the second- and third-order moments as

$$\kappa_{20} = \beta_o H_{k_p}^{k_c}(-n_o) \tag{16a}$$

$$\kappa_{02} = \beta_o H_{k_p}^{k_c}(2 - n_o) \tag{16b}$$

$$\kappa_{30} = 6\beta_i^2 G_{k_p}^{k_c}(1 - n_i, -n_i) \tag{16c}$$

$$\kappa_{12} = 2\beta_i^2[2G_{k_p}^{k_c}(1 - n_i, 2 - n_i) + G_{k_p}^{k_c}(3 - n_i, -n_i)] \tag{16d}$$

where the first and second subscripts of κ refer to the order of the height and slope, respectively, appearing in the expression. For example, the κ_{12} term is a third-order moment representing the height slope variance correlation. Also, one should note that these expressions force the height and slope variances (i.e., κ_{20} and κ_{02}) of the input and output spectra to be equal, as discussed in the previous section. For this reason, the output spectrum may be used in (16a) and (16b). Results for an inconsistent computation (where these moments are not forced to be equal) may be obtained simply by changing the subscripts i in (16c) and (16d) to o. With these definitions, the skewness parameters may then be defined as follows:

$$\lambda_{30} = \frac{\kappa_{30}}{\kappa_{20}^{3/2}} \tag{17a}$$

$$\lambda_{12} = \frac{\kappa_{12}}{\kappa_{02}\sqrt{\kappa_{20}}} \tag{17b}$$

4.3. Sea State Bias Simulation

When these skewnesses parameters enter the joint distribution of height and slopes, through a Gram-Charlier expansion, for example, the sea state bias can then be determined under the assumption of specular scattering by

$$\mathrm{SSB} = -\frac{1}{8}\left(\frac{\lambda_{30}}{3} + \lambda_{12}\right) \tag{18}$$

as discussed by *Jackson* [1979]. The first term in (18) is usually referred to as the elevation skewness bias, while the second is the electromagnetic bias.

Numerical realizations of the SSB are shown in Figure 6 where we have plotted the SSB computed from (18) as a function of the high-wavenumber cutoff k_c for $k_p = 0.20$ (rad/m) as before. The solid curve in Figure 6 shows a computation of the SSB where the second-order input and output moments have not been forced to be equal. This computation includes most of the previous SSB simulations [see, e.g., *Jackson*, 1979; *Glazman et al.*, 1996]. The dash-dotted curve, however, shows the SSB using the inverted spectrum where second-order moments are equal. One can see from Figure 6 that with the cutoff at either 40 or 3 cm (denoted in Figure 6 by *Glazman et al.* [1996] and *Jackson* [1979], respectively), the SSB from a saturated spectrum of Phillips ($5 \times 10^{-3} k^{-3}$) is about -5%. Using the inverted spectrum to compute the moments rather than the output spectrum, we find that the SSB reduces to about -1.5% for Jackson's cutoff and about -2.5% for Glazman et al.'s cutoff. The point we wish to emphasize here is not that the SSBs computed with the inverted spectrum are more correct but, rather, that these values can be significantly different from those computed under a violation of WNL theory. We believe that when short waves ($\leq$6 m) are included in the computation, the inverted spectrum must be used to preserve consistency within WNL theory. It appears that there is significant uncertainty associated with SSB quantities predicted by the studies previously mentioned. Therefore these previous studies are not correct, even though their results appear to be closer to the observed ones in terms of SSB. A complete SSB investigation must start by correctly applying the WNL theory to long gravity waves ($\lambda > 10$ m, say) and then judiciously adding intermediate and short scales. The absence of electromagnetic diffractions by shorter waves in the geometric optics model must also be investigated to determine its domain of credibility.

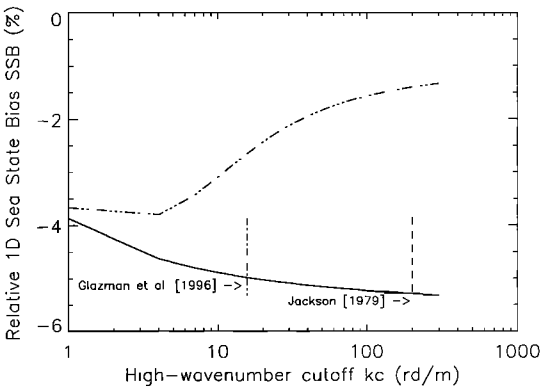

Figure 6. The relative one-dimensional sea state bias (SSB) as percent of significant wave height shown as a function of the high-wavenumber cutoff k_c in radian per meters. Solid line is obtained by applying the Phillips spectrum ($5 \times 10^{-3} k^{-3}$) at the input of the simulation by ignoring how the resulting spectrum might look at the output. The dash-dotted curve is the result of the inverted spectrum when applied at the input of the simulation in order to be consistent with the Phillips spectrum ($5 \times 10^{-3} k^{-3}$) at the output. The difference could be as high as 3% in terms of SSB.

5. Conclusion

We have shown in this paper that the theory of "weakly" nonlinear (WNL) waves as commonly used in generating higher moments of ocean-wave surface statistics has been misapplied in the calculation of the sea state bias (SSB). As a result, a pronounced inconsistency, even for lower-order moments, appears merely because the validity conditions of the theory are violated. To strictly avoid this inconsistency, only long waves must enter WNL theory. An exact extension of the theory can be made only by allowing higher-order interactions in the hydrodynamic equations. The inconsistency translates into a difference between the input and the output spectra. Even an approximate extrapolation of WNL theory cannot be achieved without an explicit inversion of the output spectrum. We have discussed how one might develop an inversion scheme that determines the required input wave spectrum for which the simulated moments remain consistent with a mea-

sured spectrum. With this procedure, shorter waves may be included even after allowing the nonlinearities to come into play. This inversion scheme is solved analytically for a one-dimensional spectrum to illustrate how divergent, in terms of the low-order spectral moments, the previous methods can be. It is also demonstrated that the inconsistency in WNL theory can have a significant impact on the calculation of SSB. The latter is highly affected by intermediate-scale waves that cannot be predicted by WNL theory. A potential use of this theory would be in the generation of nonlinear long waves that may then affect shorter-scale waves through hydrodynamic modulation.

Appendix: Definitions of Functions for the Inversion

The functions $H_{k_a}^{k_b}(\nu)$ and $G_{k_a}^{k_b}(\nu, \mu)$ are defined as single and double integrals of power functions.

$$H_{k_a}^{k_b}(\nu) = \int_{k_a}^{k_b} k^\nu \, dk = \frac{1}{\nu + 1} (k_b^{\nu+1} - k_a^{\nu+1}) \qquad \nu + 1 \neq 0 \tag{A1a}$$

$$H_{k_a}^{k_b}(\nu) = \int_{k_a}^{k_b} k^\nu \, dk = \ln (k_b/k_a) \qquad \nu + 1 = 0 \tag{A1b}$$

$$G_{k_a}^{k_b}(\nu, \mu) = \int_{k_a}^{k_b} H_{k_a}^{k}(\nu) k^\mu \, dk = \frac{1}{\nu + 1} [H_{k_a}^{k_b}(\mu + \nu + 1) - k_a^{\nu+1} H_{k_a}^{k_b}(\mu)] \qquad \nu + 1 \neq 0 \tag{A1c}$$

$$G_{k_a}^{k_b}(\nu, \mu) = \int_{k_a}^{k_b} H_{k_a}^{k}(\nu) k^\mu \, dk = T_{k_a}^{k_b}(\mu) - \ln k_a H_{k_a}^{k_b}(\mu) \qquad \nu + 1 = 0 \tag{A1d}$$

where

$$T_{k_a}^{k_b}(\mu) = \int_{k_a}^{k_b} k^\mu \ln k \, dk = \frac{k_b^{\mu+1} \ln k_b - k_a^{\mu+1} \ln k_a}{\mu + 1} - \frac{k_b^{\mu+1} - k_a^{\mu+1}}{(\mu + 1)^2} \qquad \mu + 1 \neq 0 \tag{A2a}$$

$$T_{k_a}^{k_b}(\mu) = \int_{k_a}^{k_b} k^\mu \ln k \, dk = \tfrac{1}{2} (\ln^2 k_b - \ln^2 k_a) \qquad \mu + 1 = 0 \tag{A2b}$$

Acknowledgments. The authors would like to acknowledge the helpful suggestions made by our colleagues in the Ocean Remote Sensing Group of the Applied Physics Laboratory at Johns Hopkins University. This study is funded in part by NASA's Earth Science Enterprise, Physical Oceanography Program, and the French Centre National d'Etudes Spaciales (CNES).

References

Barrick, D. E., and B. J. Lipa, Analysis and interpretation of altimeter sea echo, *Adv. Geophys.*, *27*, 60–69, 1985.

Barrick, D. E., and B. L. Weber, On the nonlinear theory for gravity waves on the ocean's surface, II, Interpretation and applications, *J. Phys. Oceanogr.*, *7*(1), 11–21, 1977.

Creamer, D. B., F. Henyey, R. Schult, and J. Wright, Improved linear representation of ocean surface waves, *J. Fluid Mech.*, *205*, 135–161, 1989.

Elfouhaily, T., B. Chapron, K. Katsaros, and D. Vandemark, A unified directional spectrum for long and short wind-driven waves, *J. Geophys. Res.*, *102*, 15,781–15,796, 1997.

Gaspar, P., F. Ogor, P.-Y. Le Traon, and O.-Z. Zanifé, Estimating the sea state bias of the TOPEX and POSEIDON altimeters from cross-over differences, *J. Geophys. Res.*, *99*, 24,981–24,994, 1994.

Glazman, R. E., and M. A. Srokosz, Equilibrium wave spectrum and sea state bias in altimetry, *J. Phys. Oceanogr.*, *21*(11), 1609–1621, 1991.

Glazman, R. E., A. Fabrikant, and M. A. Srokosz, Numerical analysis of the sea state bias for satellite altimetry, *J. Geophys. Res.*, *101*, 3789–3799, 1996.

Hasselmann, K., On the non-linear energy transfer in a gravity-wave spectrum, 1, General theory, *J. Fluid Mech.*, *12*, 481–500, 1961.

Hasselmann, K., On the non-linear energy transfer in a gravity-wave spectrum, 2, Conservation theorems; wave-particle analogy; irreversibility, *J. Fluid Mech.*, *15*, 273–281, 1962a.

Hasselmann, K., On the non-linear energy transfer in a gravity-wave spectrum, 3, Evaluation of the energy flux and swell-sea interaction for Neumann spectrum, *J. Fluid Mech.*, *15*, 385–398, 1962b.

Jackson, F. C., The reflection of impulses from a non-linear random sea, *J. Geophys. Res.*, *84*, 4939–4943, 1979.

Longuet-Higgins, M. S., The effects of non-linearities on statistical distribution in the theory of sea waves, *J. Fluid Mech.*, *17*, 459–480, 1963.

Phillips, O. M., *The Dynamics of the Upper Ocean*, 2nd ed., pp. 150, 178, Cambridge Univ. Press, New York, 1977.

Srokosz, M. A., On the joint distribution of surface elevation and slopes for a non-linear random sea, with an application to radar altimetry, *J. Geophys. Res.*, *91*, 995–1006, 1986.

Valenzuela, G. R., The growth of gravity-capillary waves in a coupled shear flow, *J. Fluid Mech.*, *76*, 229–250, 1976.

Weber, B. L., and D. E. Barrick, On the nonlinear theory for gravity waves on the ocean's surface, I, Derivations, *J. Phys. Oceanogr.*, *7*(1), 3–10, 1977.

B. Chapron, Institut Français de Recherche pour l'Exploitation de la Mer, Centre de Brest, Océanography Spatiale, 29280 Plouzané, France. (bchapron@ifremer.fr)

T. Elfouhaily and D. Thompson, Applied Physics Laboratory, Johns Hopkins University, Laurel, MD 20723. (elfoutm1@nansen.jhuapl.edu)

D. Vandemark, NASA Goddard Space Flight Center, Wallops Flight Facility, Wallops Island, VA 23337. (dug@osb.wff.nasa.gov)

(Received November 10, 1997; revised October 14, 1998; accepted December 24, 1998.)